Improving Fuzzy Algorithms for Automatic Magnetic Resonance Image Segmentation

Elnomery Zanaty and Sultan Aljahdali
College of Computer Science, Taif University, Saudi Arabia

Abstract: *In this paper, we present reliable algorithms for fuzzy k-means and C-means that could improve MRI segmentation. Since the k-means or FCM method aims to minimize the sum of squared distances from all points to their cluster centers, this should result in compact clusters. Therefore the distance of the points from their cluster centre is used to determine whether the clusters are compact. For this purpose, we use the intra-cluster distance measure, which is simply the median distance between a point and its cluster centre. The intra-cluster is used to give us the ideal number of clusters automatically; i.e a centre of the first cluster is used to estimate the second cluster, while an intra-cluster of the second cluster is obtained. Similar, the third cluster is estimated based on the second cluster information (centre and intra cluster), so on, and only stop when the intra-cluster is smaller than a prescribe value. The proposed algorithms are evaluated and compared with established fuzzy k-means and C-means methods by applying them on simulated volumetric MRI and real MRI data to prove their efficiency. These evaluations, which are not easy to specify in the absence of any prior knowledge about resulted clusters, for real MRI dataset are judged visually by specialists since a real MRI dataset cannot give us a quantitative measure about how much they are successful.*

1. Introduction

Magnetic resonance image segmentation has been proposed for a number of clinical investigations of varying complexity [33]. Automatic segmentation of MR scans is very useful for research and clinical study of much neurological pathology. The accurate segmentation of MR images into different tissue classes, especially Gray Matter (GM), White Matter (WM) and CerebroSpinal Fluid (CSF), is an important for the diagnosis and prognosis of certain illnesses. The automatic segmentation of brain MR images, however, remains a persistent problem. The major MR image segmentation problem when MR image is the corruption with an inhomogeneity bias field [11]. Several approaches have been proposed to address this limitation of intensity-based classification under three broad algorithmic frameworks, namely, region-based, contour-based, and classification-based approaches.

In region-based segmentation, the shape of an object can be described in terms of its boundary or the region it occupies. In its simplest form, region growing methods usually start by locating some seeds representing distinct regions in the image [33, 11]. The seeds are then grown until they eventually cover the entire image. The region growing process is therefore governed by a rule that describe the growth mechanism and a rule that check the homogeneity of the regions at each growth step. Region growing technique has been applied to MRI segmentation [11, 24, 20]. In [11], a semi-automatic, interactive MRI segmentation algorithm was developed that employ simple region growing technique for lesion segmentation. In [24], an automatic statistical region growing algorithm based on a robust estimation of local region mean and variance for every pixel on the image was proposed for MRI segmentation. The best region growing parameters are automatically found via the minimization of a cost functional. Furthermore, relaxation labeling, region splitting, and constrained region merging were used to improve the quality of the MRI segmentation. The determination of an appropriate region homogeneity criterion is an important factor in region growing segmentation methods. However, such homogeneity criterion may be difficult to obtain a priori. In [20], an adaptive region growing method was proposed where the homogeneity criterion is learned automatically from characteristics of the region to be segmented while searching for the region. Contour-based segmentation approach assumes that the different objects in an image can be segmented by detecting their boundaries. A contour-based segmentation is based on the deformable templates or active contours [12, 17, 2, 18, 8]. Active contour deforms to fit the object's shape by minimizing (among others) a gradient dependent attraction force while at the same time maintaining the smoothness of the contour shape [12]. Active contour based algorithms usually require initialization of the contour close to the object boundary for it to converge successfully to the true boundary. More importantly, active contour methods have difficulty handling deeply

convoluted boundary such as CSF, GM and WM boundaries due to their contour smoothness requirement [17]. Hence, they are often not appropriate for the segmentation of brain tissues. Nevertheless, it has been applied successfully to the segmentation of intracranial boundary [2], brain outer surface [18], and neuro-anatomic structures in MR brain images [8]. In classification-based segmentation, pixels are classified and labeled as belonging to a particular tissue class according to a certain criterion. The simplest technique is based on thresholding [23, 21, 29, 19, 16, 30, 1, 31]. Thresholding algorithm attempts to determine a threshold value which separates the desired classes. In [23], Suzuki and Toriwaki used iterative thresholding to distinguish brain tissues from others in axial MR slices. Starting at set values, thresholds for the head and the brain are then iteratively adjusted based on the geometry of resulting masks. In [21], Rajapakse *et al*. also used the Gaussian mixture to model the three brain tissue classes. The biological variations of a particular tissue class are accounted for in their statistical model by assuming that the mean intensities of the tissue classes are slowly varying spatial functions. Common others classification techniques include clustering algorithms [29, 9, 16], decision fusion [30], and artificial neural network and support vector machines [1, 31].

Clustering, from a machine learning perspective, is a popular unsupervised classification method and has found many applications in pattern classification and image segmentation [4, 14, 13, 22, 25, 10, 15]. Clustering algorithm attempts to classify a voxel to a tissue class by using the notion of similarity to the class. Clustering techniques require the definition of a similarity measure between pixels, which is not easy to specify in the absence of any *prior* knowledge about cluster shapes. The Fuzzy C-Means (FCM) clustering algorithms have recently been applied to MRI segmentation [10, 15]. Unlike the crisp *k*-means clustering algorithm [4, 14, 13, 22, 25], the FCM algorithm allows partial membership in different tissue class. Thus, FCM can be used to model the partial volume averaging artifact, where a pixel may contain multiple tissue classes [10]. A method of simultaneously estimating the intensity non-uniformity artifact and performing voxel classification based on fuzzy clustering has been reported in [15], where intermediate segmentation results are utilized for the intensity non-uniformity estimation. The method uses a modified FCM cost functional to model the variation in intensity values and the computation of the bias field is formulated as a variation problems. However, in conventional FCM clustering algorithm, there is no consideration of spatial context between voxels since the clustering is done solely in the feature space. Although *k*-means and *C*-means methods have several advantages such as: (1) it yields regions more homogeneous than those of other methods, (2) it

reduces the spurious blobs, (3) it removes noisy spots, and (4) it is less sensitive to noise than other techniques. The final number of clusters is still always sensitive to one or two user-selected parameters that define the threshold criterion for merging. Though some compatibility or similarity measure can be applied to choose the clusters to be merged, no validity measure is used to guarantee that the clustering result after a merge is better than the one before the merge. Partial results were stated in [9] to answer the questions: "Can the appropriate number of clusters be determined automatically? And if the answer is yes, how?" The number of clusters is determined by operating index procedures to whole data to determine the number of clusters before starting fuzzy methods. This will consume much time for finding the suitable number of cluster. Therefore, two major problems are known with the *k*-means and FCM methods: (1) How to determine the number of clusters. (2) The computational cost is quit high for large data sets.

This paper addresses these problems for overcoming the shortcomings of existing fuzzy methods. We present alternative k-means and FCM algorithms that could improve MRI segmentation. The algorithms incorporate spatial information into the membership function and the validity procedure for clustering. We use the intra-cluster distance measure, which is simply the median distance between a point and its cluster centre. The number of the cluster increases automatically according the value of intra-cluster, for example when a cluster is obtained, it uses this cluster to evaluate intra-cluster of the next cluster as input to the FCM or k-means and so on, stop only when intra-cluster is smaller than a prescribe value. The most important aspect of the proposed algorithms is actually to work automatically. Alterative is to improve automatic image segmentation. The performance of the proposed method is illustrated using simulated volumetric MRI and real MRI. Due to the reference of real MRI dataset being unknown to measure how much our algorithms are successful, the opinion of specialists are considered. The rest of this paper is organized as follows. Section 2 describes the MRI segmentation problem. The proposed k-means clustering algorithm and fuzzy c-means are presented in sections 3, 4, respectively. Experimental comparisons are given in section 5. Finally, section 6 gives our conclusions.

2. The MRI Segmentation Problem

The basic idea of image segmentation can be described as follows. Given a set of data $X = \{x_1, x_2, \ldots x_N\}$ and a uniformity predicate P, we wish to obtain a partition of the data into disjoint nonempty groups $\{v_1, v_2, \ldots, v_k\}$ subject to the following conditions:

a. $\bigcup_{i=1}^{k} v_i = X$

b. $v_i \cap v_j = \varphi, \quad i \neq j$

c. $P(v_i) = True, \quad i = 1, 2 \ldots, k$

d. $P(vi \cup vj) = False, \quad i \neq j$

The first condition ensures that every data value must be assigned to a group, while the second condition ensures that a data value can be assigned to only one group. The third and fourth conditions imply that every data value in one group must satisfy the uniformity predicate while data values from two different groups must fail the uniformity criterion. To obtain a 3D MR image, the positional information about the tissues must be recorded. This involves isolating the source of each component of the MR signal to a particular voxel using the technique of spatial encoding [10, 3]. In MR imaging, spatial encoding is achieved by performing slice selection in one direction (e.g. the z-axis), frequency encoding in another direction (e.g. the x-axis), and phase encoding in the third direction (e.g. the y-axis). In slice selection, a narrow bandwidth is applied in the presence of a z-axis linear gradient field. Since the resonance frequency of a proton is proportional to the applied magnetic field, the presence of a gradient field means that only a narrow slice in the body will have a resonant frequency within the bandwidth of the resonant frequency [7, 6]. The MR image segmentation involves the separation of image pixels into regions comprising different tissue type. All MR images are affected by random noise. The noise comes from the stray current in the detector coil due to the fluctuating magnetic fields arising from random ionic currents in the body, or the thermal fluctuations in the detector coil itself, more discussion can be seen [26]. When the level of noise is significant in an MR image, tissues that are similar in contrast could not be delineated effectively, causing error in tissue segmentation. Then more sophisticated techniques would be needed to reconstruct the image from incomplete information [27, 28, 5]. A 3D image can be obtained from many consecutive 2D slices.

3. The Proposed *k*-Means Clustering Algorithm

K-means clustering is one of the simplest unsupervised classification algorithms [4, 13, 14]. The procedure follows a simple way to classify the dataset through a certain number of clusters. The algorithm partitions a set of N vector $X = \{x_j, j = 1, \ldots, N\}$ into C classes $v_i, i = 1, \ldots, C$, and finds a cluster centre for each class c_i denotes the centroid of cluster v_i such that an objective function of dissimilarity, for example a distance measure, is minimized. The objective function that should be minimized, when the Euclidean distance

is selected as a dissimilarity measure, can be described as:

$$P = \sum_{i=1}^{C} \left(\sum_{k, x_k} \|x_k - c_i\|^2 \right) \tag{1}$$

where $\sum_{k, x_k} \|x_k - c_i\|^2$ is the objective function within group i, and $\|x_k - c_i\|$ is a chosen distance measure between a data point x_k and the cluster centre c_i. The partitioned groups are typically defined by a $(C \times N)$ binary membership matrix $U = (u_{ij})$, where the element u_{ij} is 1 if the jth data point x_j belongs to group i, and 0 otherwise. This means:

$$u_{ij} = \begin{cases} 1 & if \|x_j - c_i\|^2 \leq \|x_j - c_k\|^2 \quad \forall k \neq i \\ 0 & otherwise \end{cases} \tag{2}$$

$$c_i = \frac{\sum_{j=1, x_j \in c_i}^{N} x_j}{R_i} \tag{3}$$

where R_i is number of data point in class v_i. Since the *k*-means method aims to minimize the sum of squared distances from all points to their cluster centers, this should result in compact clusters. We use the intra-cluster distance measure, which is simply the median distance between a point and its cluster centre. The equation is given as:

$$Intra = midean \left(\sum_{i=1}^{C} \sum_{x \in ci} \|x - v_i\|^2 \right) \tag{4}$$

Therefore, the clustering which gives a minimum value for the validity measure will tell us what the ideal value of k is in the *k*-means. Then the number of cluster is known before estimating the membership matrix. The proposed *k*-means clustering algorithm is described as follows:

1. Select a subset from the dataset instead of using all of them.
2. Set $C = 2$ the initial number of cluster, and C_{max} = the maximum number of cluster (it is selected arbitrary).
3. Determine the membership matrix U according to equation 2 using C is set C_{max}.
4. Compute the objective function according to equation 1. Go to step 6, if either it is below a certain tolerance value or its improvement over previous iteration is below a certain threshold.
5. Update the cluster centers $c_i, i = 1, \ldots, C$ using equation 3, then go to step 3.
6. Obtain the center v_1.

7. Apply step 3 and use v_1 centers as input c number of cluster to obtain center v_2.

8. Use v_2 to calculate the intra distance according to the equation 4. Stop if intra is smaller than a prescribe value else set $C = C+1$, return to step 3, until $C = C_{max}$.

4. The Proposed Fuzzy C-Means Algorithm

Fuzzy C-means (FCM) clustering, also known as fuzzy ISODATA, is a data clustering algorithm in which each data point belongs to a cluster to determine a degree specified by its membership grade. Bezdek [4, 13, 14] has proposed this algorithm as an alternative to earlier *k*-means clustering. FCM partitions a collection of N vector x_i, $i = 1,\dots,N$ into C fuzzy groups, and finds a cluster centre in each group such that an objective function of a dissimilarity measure is minimized. The major difference between FCM and *k*-means is that FCM employs fuzzy partitioning such that a given data point can belong to several groups with the degree of belongingness specified by membership grades between 0 and 1. In FCM, the membership matrix U is allowed to have not only 0 and 1 but also the elements with any values between 0 and 1. This matrix satisfies the constraints:

$$\sum_{i=1}^{C} u_{ij} = 1, \quad \forall j = 1,\dots,N \tag{5}$$

The objective function of FCM can be formulated as follows:

$$p(u,v_1,\dots v_c) = \sum_{i=1}^{C}\sum_{j=1}^{N} u_{ij}^{m} \left\| x_j - c_i \right\|^2 \tag{6}$$

where ui_j is between 0 and 1, c_i is the cluster centre of fuzzy group i, and the parameter m is a weighting exponent on each fuzzy membership (in our implementation, we set it to 2). Fuzzy partitioning is carried out through an iterative optimization of the objective function shown above, updating of membership u_{ij} and the cluster centers c_j by:

$$c_i = \frac{\sum_{j=1}^{N} u_{ij}^{m} x_j}{\sum_{j=1}^{N} u_{ij}^{m}} \tag{7}$$

$$u_{ij} = \frac{1}{\sum_{k=1}^{C}\left(\frac{\left\| x_j - c_i \right\|}{\left\| x_j - c_k \right\|}\right)^{2/(m-1)}} \tag{8}$$
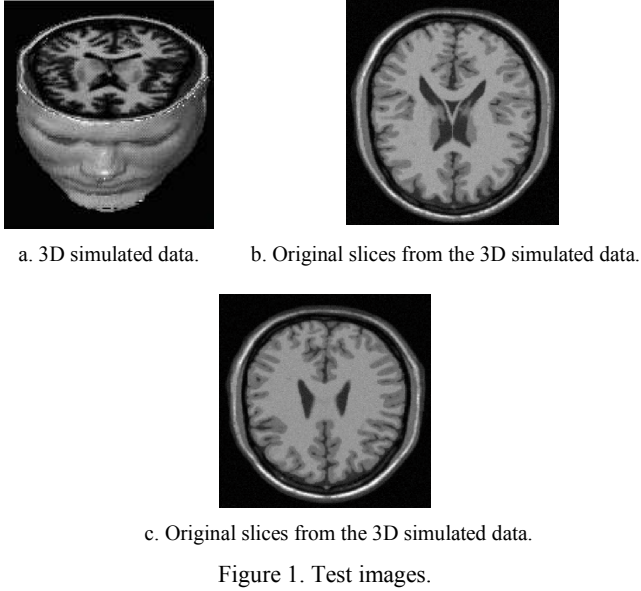
Simlar to *k*-means method, we use the intra-cluster distance measure, which is simply the median distance between a point and its cluster centre as shown in equation 4. The proposed algorithm is described as follows:

1. Select a subset from the dataset.
2. Set $C = 2$ the initial number of cluster, and C_{max} =the maximum number of cluster (it is selected arbitrary).
3. Initialize the membership matrix U with random values between 0 and 1 such that the constraints in Equation 5 are satisfied.
4. Calculate fuzzy cluster centers c_i, $i = 1,\dots,C$ using Equation 7.
5. Compute the objective function according to Equation 6. Go to step 7, if either it is below a certain tolerance value or its improvement over previous iteration is below a certain threshold.
6. Compute a new membership matrix U using Equation 8, then go to step 2.
7. Obtain the center v_1.
8. Apply step 3 on the subset with c number of cluster to obtain center v_2.
9. Use v_2 to calculate the intra distance according to the Equation 4. Stop if intra is smaller than a prescribe value else set $C = C+1$, return to step 3, until $C = C_{max}$

5. Experimental and Comparative Results

The experiments were performed with several data sets on a PC with a P4 2.4GHZ CPU, 256 MB of RAM and performed in MATLAB. Our expremint includes one on simulated MR and another on real MR brain data consisting of several classes. The advantages of using digital phantoms rather than real image data for validating segmentation methods include prior knowledge of the true tissue types and control over image parameters such as modality, slice thickness, noise and intensity inhomogeneities. We used a high-resolution T1-weighted MR phantom with slice thickness of 1mm, 3% noise and no intensity inhomogeneities, obtained from the classical simulated brain database of McGill University [5]. Two transverse slices drawn from the simulated MR data are shown in Figure 1. MRI has several advantages over other imaging techniques enabling it to provide 3-dimensional data with high contrast between soft tissues (see Figures 1(a)). However, the amount of data is far too much for manual analysis/interpretation, and this has been one of the biggest obstacles in the effective use of MRI. Segmentation of MR images into different tissue classes, especially Gray Matter (GM),

White Matter (WM) and CerebroSpinal Fluid (CSF), is an important task. Brain MR-images have a number of features, especially the following: Firstly, they are statistically simple: MR Images are theoretically piecewise constant with a small number of classes. Secondly, they can have relatively high contrast between different tissues. Unlike many other medical imaging modalities, the contrast in an MR image depends strongly upon the way the image is acquired.

a. 3D simulated data.   b. Original slices from the 3D simulated data.

c. Original slices from the 3D simulated data.

Figure 1. Test images.

The quality of the segmentation algorithm is of vital importance to the segmentation process. The comparison score S for each algorithm is proposed in [32], which defined as:

$$S = \left| \frac{A \cap A_{ref}}{A \cup A_{ref}} \right| \qquad (13)$$

where A represents the set of pixels belonging to a class as found by a particular method and A_{ref} represents the set of pixels belonging to the very same class in the reference segmented image (ground truth).

5.1. MRI Segmentation Results

Here we compare the evaluation of our proposed methods to the standard Fuzzy *k*-means and C-Means (FCM) methods when they are applied to simulated MR and real MR data.

5.1.1. Experiment on the Simulated MR Data

Table 1 shows the corresponding average percentage of accuracy scores of the individual segmentation methods, after applying them to the simulated MR data (two slices of the segmented 3D MR volume). The volume was reduced in size to $181 \times 108 \times 90$ to reduce the high computational cost. A qualitative representation of the segmentation results is shown in

Figures 2 and 3 The Figures show two slices of the segmented 3D MR volume.

5.1.2. Experiment on the Real MR Data

Table 2 shows the corresponding accuracy scores of the four methods for the nine classes of real images (real brain image with nine classes, for example see class 0 in Figure 1(a)). Obviously, the proposed k-means and FCM methods are more stable and achieve much better performance than the others for most classes. Another advantage our methods work automatically while in the standard k-means and FCM, the number of cluster is manually determined.

Table 1. Segmentation accuracy (%) of eight methods on brain classes.

Methods	Accuracy of MRI Volume
K-means	0.55394
The proposed k-means	0.58341
FCM	0.52531
The proposed FCM	0.604318

a. K-means.   b. FCM.

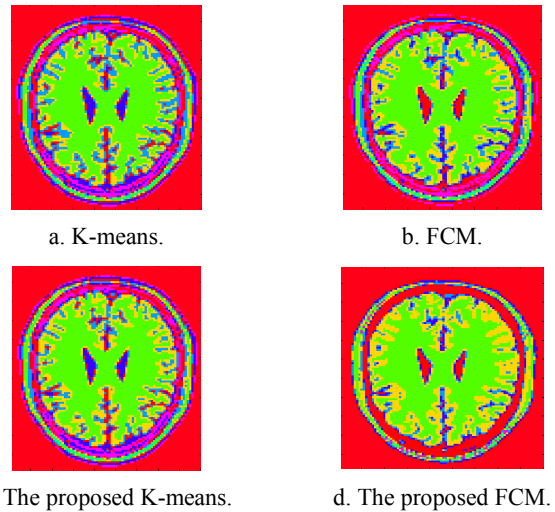c. The proposed K-means.   d. The proposed FCM.

Figure 2. Segmentation results for the slice (*z*=100) on a simulated data using methods.

5.2. Specialists Judgment

In this section, two real T2-weigthed MRI images (data1 and data2) are obtained as test sets from the x-ray Department, Faculty of Medicine as shown in Figure 5. The anatomical model used to generate real brain MRI data consist of tissue volumes, one for each tissue class WM within the brain parenchyma, GM within the brain parenchyma, CSF surrounding the brain and within the ventricles, FAtty Tissue (FAT), Skull bone (does not include sinuses), SKN (mostly skin). The voxel value in these volumes reflects the proportion of tissue presented in the voxel, in the range [0, 255] as shown in Figure 4.

The opinions of five medical doctors in PhD degree have taken have knowledge about number of clusters

in the images. Which each slice with six classes and consisting of 384×512 pixels. Qualitative representation of the segmentation results for two real MRI image are shown in Figures 6 and 7, using the segmentation methods. The application of these algorithms to a real MRI dataset cannot give us a quantitative measure about how they are successful. As such, qualitative assessment of the segmentation results is judged visually.

The qualitative comparison results of the segmented image methods are represented in Table 3, where the opinion of doctors from x-ray department has been considered. In case data2, all of doctors show that the proposed methods give better results, as shown in Table 3, which a value/reference of the proposed FCM is the best and the established *k*-means is the worst method. After that, the standard FCM, and *k*-means methods respectively misclassified some parts of gray matter into white matter. In contrast, the proposed

methods can yield satisfactory result, which is more compatible with human visual perception. On the other hand, data1 more complicated than data2, so the judge on this data become more difficult. In this case, all doctors show that the proposed FCM segmentation method gives better results. Although, the proposed *k*-means, standard FCM, and *k*-means methods, respectively misclassified some parts of gray matter into white matter. The proposed method is still obtained better results than standard FCM, and *k*-means methods. We rearrange the reference according to majority of doctors after seeing the different results as shown in Figure 6, which the rank total is computed through, computed the average percentage between the two data when using one method. The percentage is assumed, which reference 1, 2,...,6 take percentage 60, 50,...,10, respectively.

Table 2. Segmentation accuracy (%) of eight methods on brain classes.

Method	Class 1	Class 2	Class 3	Class 4	Class 5	Class 6	Class 7	Class 8	Class 9	Overall
K-means	62.96	57.53	77.84	91.61	66.47	77.18	85.96	43.6	99.15	77.36
FCM	53.52	64.38	75.19	89.3	62.76	29.09	83.09	6.76	98.95	73.73
The proposed k-means	67.55	61.14	78.83	100.0	67.96	61.87	89.21	51.27	97.27	66.55
The proposed FCM	64.92	87.64	77.84	86.18	66.17	89.18	99.95	20.3	99.03	80.46

a. K-means.

b. FCM.

c. The proposed K-means.

d. The proposed FCM.

Figure 4. Segmentation results for the slice (z=91) on a simulated data using methods.

Table 3. The rank of data1 and data2.

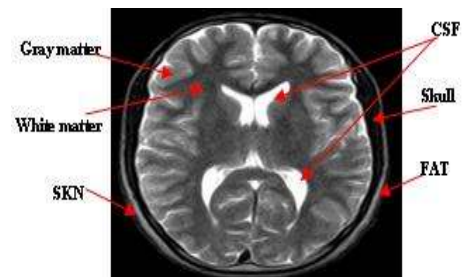| Method	Rank Data1	Rank Data2	Rank Total
k-means	1	2	2
FCM	2	3	3
The proposed K-means	2	1	1
The proposed FCM	1	1	1
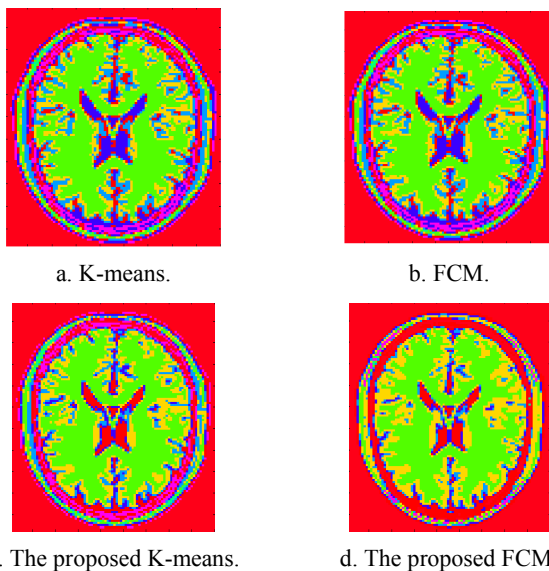
Figure 4. The anatomical model for real MRI image.
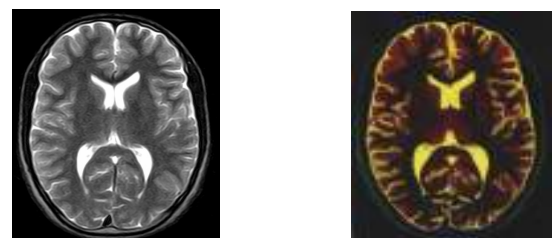
a. Original image of data1 image.

b. manual segmentation of the image shown in 5(a).
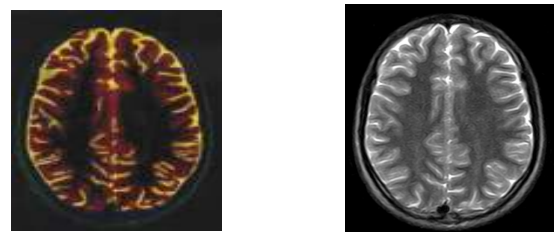
c. Original image of data2 image.

d. manual segmentation of the image shown in 5(c).

Figure 5. MRI image.

a. k-means.

b. FCM.

c. The proposed k-means.

d. The proposed FCM.
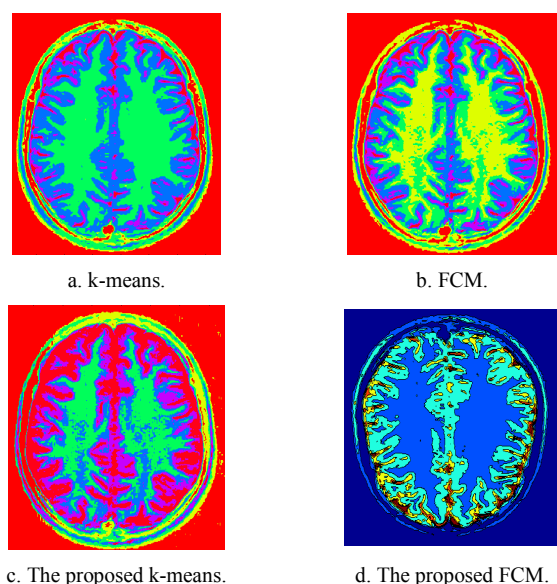
Figure 6. Segmentation of real MRI image (data2).

a. k-means.

b. FCM.

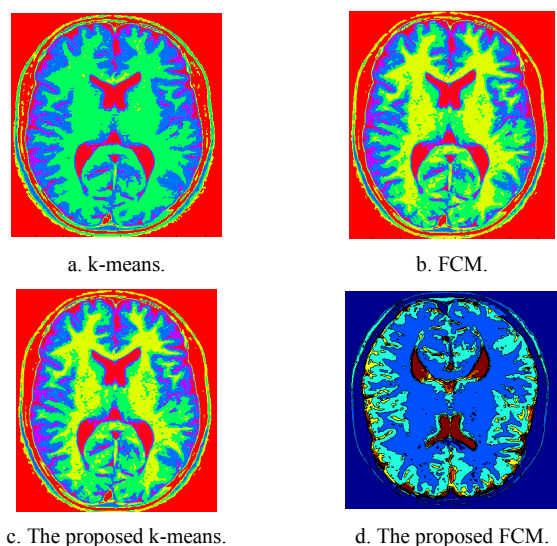c. The proposed k-means.

d. The proposed FCM.

Figure 7. Segmentation of real MRI image (data1).

6. Conclusions

A method for improving image segmentation has been presented. Rather than tuning a method for the best possible performance. It works automatically and can indeed improve the segmentation accuracy over the existing methods. The algorithms incorporate spatial information into the membership function and the validity procedure for clustering. They have estimated accurate clusters automatically even without knowing prior knowledge of the true tissue types and the number of cluster of given images.

Extensive experiments using MR images generated by the Brain Web simulator [5] and real MR data have been used to evaluate the proposed methods. Due to the use of soft segmentation, the proposed FCM algorithm is able to give a good estimation of tissue volume in the presence of inaccurate tissues.

In the case of real MR images, although the proposed K-means method misclassified some parts of gray matter into white matter, it is still achieve better

results than the standard K-means and C-means. By comparing the proposed methods with established one, it is clear that our algorithms can estimate the correct tissues much more accurately than the established algorithms. Furthermore, the proposed methods to clustering turn out to be particularly interesting because, due to partial volume effects during acquisition, pixel values at the borders between volumes of interest correspond to mixtures of different anatomical tissues.

Future research in MRI segmentation should strive toward improving the accuracy, precision, and computation speed of the segmentation algorithms, while reducing the amount of manual interactions needed. This is particularly important as MR imaging is becoming a routine diagnostic procedure in clinical practice. It is also important that any practical segmentation algorithm should deal with 3D volume segmentation instead of 2D slice by slice segmentation, since MRI data is 3D in nature.

Acknowledgments

References

[1] Alirezaie J. and Jernigan ME., "MR Image Segmentation and Analysis Based on Neural Networks," *in Signal Processing for Magnetic Resonance Imaging and Spectroscopy*, Marcel Dekker, pp. 341-364, 2002.

[2] Atkins M. and Mackiewich B., "Fully Automatic Segmentation of the brain in MRI," *in Proceedings of IEEE Transaction,* vol. 17, pp. 98-107, 1998.

[3] Bedell B. and Narayana P., "Automatic Segmentation of Gadoliniumenhanced Multiple Sclerosis Lesions," *Magnetic Resonance in Medicine*, vol. 39, pp. 935-940, 1998.

[4] Bezdek J., "Pattern Recognition with Fuzzy Objective Function Algorithms," *Plenum Press*, New York, 1981.

[5] Brain W., "Simulated Brain Database," *McConnell Brain Imaging Centre*, Montreal Neurological Institute, McGill,Canada, .

[6] Buxton R., "Introduction to Functional Magnetic Resonance Imaging-Principles and Techniques," Cambridge University Press, 2002.

[7] Chakeres D. and Schmalbrock P., *Fundamentals of Magnetic Resonance Imaging*, Williams and Wilkins, 1992.

[8] Duta N. and Sonka M., "Segmentation and Interpretation of MR Brain Images: An

Improved Active Shape Model," *in Proceedings of IEEE Transaction Medical Imag*, vol. 17, pp. 1049-1062, 1998.

[9] El-Melegy M., Zanaty E., Abd-Elhafiez M., and Farag A., "On Cluster Validity Indexes in Fuzzy and Hard Clustering Algorithms for Image Segmentation," *in Proceedings of IEEE International Conference on Computer Vision*, vol. 6, pp. 5-8, 2007.

[10] Haacke E., Brown R., Thompson M., and Venkatesan R., *Magnetic Resonance Imaging: Physical Principles and Sequence Design*, Wiley, 1999.

[11] Heinonen T., Dastidar P., Eskola H., Frey H., Ryymin P., and Laasonen E., "Applicability of Semi-Automatic Segmentation for Volumetric Analysis of Brain Lesions," *Journal of Medical Engineering and Technology*, vol. 22, pp. 173-178, 1998.

[12] Ji L. and Yan H., "An Attractable Snakes Based on the Greedy Algorithm for Contour Extraction," *Pattern Recognition*, vol. 35, no. 4, pp. 791-806, 2002.

[13] Liew A., Leung S., and Lau W., "Fuzzy Image Clustering Incorporating Spatial Continuity," *IEEE Proceedings Vision, Image, and Signal Processing*, vol. 147, no. 2, pp. 185-192, 2000.

[14] Liew A., Leung S., and Lau W., "Segmentation of Color Lip Images by Spatial Fuzzy Clustering," *IEEE Transactions on Fuzzy System*, vol. 11, no. 4, pp. 542-549, 2003.

[15] Liew A. and Yan H., "An Adaptive Spatial Fuzzy Clustering Algorithm for MR Image Segmentation," *IEEE Transactions on Medical Imaging*, vol. 22, no. 9, pp. 1063-1075, 2003.

[16] Liew A. and Yan H., "Current Methods in the Automatic Tissue Segmentation of 3D Magnetic Resonance Brain Images," *Medical Imaging Reviews*, Bentham Science Publishers, vol. 2, no. 1, pp. 91-103, 2006.

[17] McInerney T. and Terzopoulos D., "Deformable Models in Medical Image Analysis: A Survey," *Medical Image Analysis*, vol. 1, pp. 91-108, 1996.

[18] Michailovich O., Rathi Y., and Tannenbaum A., "Image Segmentation Using Active Contours Driven by the Bhattacharyya Gradient Flow," *IEEE Transactions on Image Processing*, vol. 16, no. 11, pp. 2787-2801, 2007.

[19] Phamv D. and Prince J., "Adaptive Fuzzy Segmentation of Magnetic Resonance Images," *IEEE Transactions on Medical Imaging*, vol. 18, no. 9, pp. 737-751, 1999.

[20] Pohle R. and Toennies K., "Segmentation of Medical Images Uses Adaptive Region Growing," *in Proceedings of SPIE Medical Imaging 2001*, San Diego, pp. 1322-1337, 2001.

[21] Rajapakse J., Giedd J., and Rapoport J., "Statistical Approach to Segmentation of Single-Channel Cerebral MR Images," *IEEE Transactions on Medical Imaging*, vol. 16, no. 2, pp. 176-86, 1997.

[22] Szeto L., Liew A., Yan H., and Tang S., "Gene Expression Data Clustering and Visualization Based on a Binary Hierarchical Clustering Framework," Special issue on "Biomedical Visualization for Bioinformatics," *Journal of Visual Languages and Computing*, vol. 14, pp.341-362, 2003.

[23] Suzuki H. and Toriwaki J., "Automatic Segmentation of Head MRI Images by Knowledge Guided Thresholding," *Computerized Medical Imaging and Graphics*, vol. 15, no. 4, pp. 233-240, 1991.

[24] Tamez-Pena J., Totterman S., and Parker K., "Unsupervised Statistical Segmentation of Multispectral Volumetric MR Images," *in Proceedings of SPIE (Medical Imaging 1999)*, San Diego, pp. 3661-3371, 1999.

[25] Wu S ., Liew A., and Yan H., "Cluster Analysis of Gene Expression Data Based on Self-Splitting and Merging Competitive Learning," *IEEE Transactions on Information Technology in Biomedicine*, vol. 8, pp. 5-15, 2004.

[26] Yan H. and Gore J., "An Efficient Algorithm for MR Image Reconstruction Without Low Spatial Frequencies," *IEEE Transactions on Medical Imaging*, TMI-9, pp. 184-179, 1990.

[27] Yan H. and Braun M., "Image Reconstruction from Fourier Domain Data Sampled Along a Zig-Zag Trajectory," *Magnetic Resonance in Medicine*, vol. 18, pp. 405-410, 1991.

[28] Yan H., *Signal Processing in Magnetic Resonance Imaging and Spectroscopy*, Marcel Dekker, 2002.

[29] Zanaty E., "Comparison Between Classical and Clustering Segmentation Techniques," *ICIS Journal*, pp. 75-98, 2007.

[30] Zanaty E., El-Melegy M., and Abd-Elhafiez M., "Improving Image Segmentation Via Decision Fusion," *Egyptian Informatics Journal*, 2008.

[31] Zanaty E. and Aljahdali S., "Improving the Accuracy of Support Vector Machines," *in Proceedings of 23rd International Conference on Computers and Their Application,* pp. 111-115, Cancun, Mexico, 2008.

[32] Zhang D., Chen S., "A Novel Kernelized Fuzzy C-Means Algorithm with Application in Medical Image Segmentation," *Artificial Intelligence in Medicine*, vol. 32, pp. 37–50, 2004.

[33] Zhang H., Fritts J., and Goldman S., "Image Segmentation Evaluation: A Survey of Unsupervised Methods," *Computer Vision and*

Image Understanding (CVIU), vol. 110, no. 2, pp. 260-280, 2008.

Elnomery Zanaty is an associate professor at Taif University, Saudi Arabia. He received his MSC degree in computer science in 1997 from South Valley University, Egypt. He completed his PhD studies at TU-Chemnitz, Germany, during the period 2000-2003. His research interests are reverse engineering, data reduction, image segmentation, and image reconstruction. He has published over 20 technical papers in refereed international journals or conference proceedings.

Sultan Aljahdali had his BSc from Winona State University, Winona, Minnesota in 1992, and MS with honor from Minnesota State University, Mankato, Minnesota, 1996, and PhD information Technology from George Mason University, Fairfax, Virginia, USA, 2003. Dr. Aljahdali is dean of the college of Computers and Information Systems at Taif University. His research interest includes software testing, developing software reliability models, soft computing for software engineering, computer security, reverse engineering, and medical imaging. Furthermore, he is a member of ACM, IEEE, and ISCA.